polymers

MDPI

Article

Efficient Production of Poly(Cyclohexene Carbonate) via ROCOP of Cyclohexene Oxide and CO_2 Mediated by NNO-Scorpionate Zinc Complexes

Sonia Sobrino[1], Marta Navarro[2], Juan Fernández-Baeza[1,*], Luis F. Sánchez-Barba[2,*], Agustín Lara-Sánchez[1], Andrés Garcés[2], José A. Castro-Osma[1] and Ana M. Rodríguez[1]

[1] Universidad de Castilla-La Mancha, Departamento de Química Inorgánica, Orgánica y Bioquímica- Centro de Innovación en Química Avanzada (ORFEO-CINQA), Campus Universitario, 13071-Ciudad Real, Spain; Sonia.Sobrino@uclm.es (S.S.); Juan.FBaeza@uclm.es (J.F-B.); Agustin.Lara@uclm.es (A.L-S.); JoseAntonio.Castro@uclm.es (J.A.C-O.); AnaMaria.RFdez@uclm.es (A.M.R.F.)

[2] Departamento de Biología y Geología, Física y Química Inorgánica, Universidad Rey Juan Carlos, Móstoles-28933-Madrid, Spain; marta.navarro.sanz@urjc.es (M.N.); luisfernando.sanchezbarba@urjc.es (L.F.S-B.); andres.garces@urjc.es (A.G.)

* Correspondence: luisfernando.sanchezbarba@urjc.es; Tel.: +34-91-488-8504

Received: date; Accepted: date; Published: date.

Published article available at https://www.mdpi.com/2073-4360/12/9/2148

Abstract: New mono- and dinuclear chiral alkoxide/thioalkoxide NNO-scorpinate zinc complexes have been easily synthesized in very high yields, and characterized by spectroscopic methods. X-ray diffraction analysis unambiguously confirmed the different nuclearity of the new complexes as well as the variety of coordination modes of the scorpionate ligands. Scorpionate zinc complexes **2**, **4** and **6** were assessed as catalysts for polycarbonate production from epoxide and carbon dioxide with no need of a co-catalyst or activator under mild conditions. Interestingly, at 70 °C, 10 bar of CO_2 pressure and 1 mol% of loading, the dinuclear thioaryloxide [Zn(bpzaepe)$_2${Zn(SAr)$_2$}] (**4**) behaves as an efficient and selective one-component initiator for the synthesis of poly(cyclohexene carbonate) via ring-opening copolymerization of cyclohexene oxide and CO_2, affording polycarbonate materials with narrow dispersity values.

Keywords: Scorpionate zinc complexes, ring-opening copolymerization (ROCOP), CO_2 fixation, poly(cyclohexene carbonate) production.

1. Introduction

Over the last decade the conversion of carbon dioxide (CO_2) into commercially viable commodities has attracted great interest in the scientific community, since carbon dioxide represents a real alternative carbon feedstock for a sustainable chemical industry [1,2].

CO_2 is an attractive C-1 renewable building block [3] given its abundance in nature, low cost, non-toxicity, lack of colour and redox activity. Many chemical transformations are possible for this unsaturated molecule, however, the selective production of cyclic carbonates or polycarbonates through the cycloaddition or the ring-opening copolymerization (ROCOP) of CO_2 with epoxides, respectively, (see Scheme 1) is gaining high attention as a 100% atom-economy route to convert waste CO_2 into valuable materials [4,5].

Thus, cyclic carbonates present important applications as electrolytes, engineering plastics, solvent, fuel additives, and precursors to fine chemicals [6], whereas polycarbonates incorporate very smart physical features, such as durability, moldability, lightness, transparency and impact resistence

[7], in addition to their biodegradability and biocompatibility that make them highly attractive in the biomedical field [8,9].

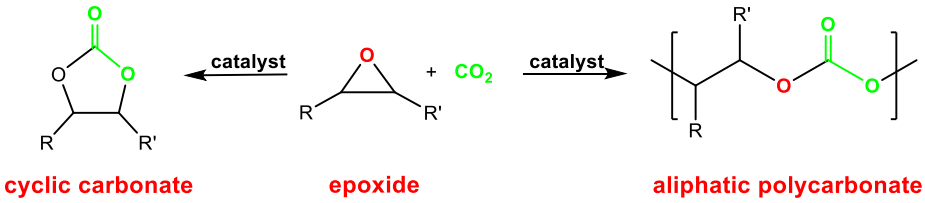

Scheme 1. Synthesis of cyclic and polycarbonates.

Particularly, the structures of the resulting polycarbonates, which can include up to 50% of carbon dioxide in the polymer backbone, will determine their future applications. For instance, non-isocyanate polyurethanes (NIPUs) can be prepared employing low molar mass hydroxyl-telechelic polycarbonates [10,11], whereas higher molar mass CO_2-derived polycarbonates find numerous applications as engineering polymers, packaging plastics, elastomers, adhesives and coatings [12].

Nevertheless, given the high thermodynamic stability and kinetic inertness of the CO_2 molecule [13], the environmental and economical viability of the ROCOP depends on the capability of the catalytic system to avoid high temperatures and pressures [14], which should be able, in turn, to operate at ambient temperatures and pressures [15] as well as controlling rates and polymer molecular weight and composition [16]. In this context, very active and selective metal-based catalysts have been successfully developed for the ROCOP of carbon dioxide and epoxides, frequently in the presence of a nucleophile as co-catalyst, with zinc [17-25], chromium [26,27], cobalt [28-29], iron [30,31], rare earth metals [32,33] and aluminum [34,35] as dominating metals in this field, although non-metal and organocatalyst systems have been also recently reported [36]. Similarly, very efficient bimetallic systems have been also reported for the selective copolymerization of epoxides and carbon dioxide, in which the epoxide is activated by one metal, while the attacking nucleophile is provided by the second centre [37,38].

Considering the current potential large-scale production of aliphatic polycarbonates by a number of companies [39-41], the employment of biocompatible metals such as zinc [42,43] is highly desirable to avoid potential health issues related to the toxicity of several metal-based residues in the isolated copolymers [44,45]. Particularly, very active zinc-based catalysts in the absence of co-catalyst have been described [17-25] for polycarbonate production, some of them including alkoxide, amide, alkyl and acetate ligands as nucleophile in a coordination-insertion mechanism (see Chart 1).

On the other hand, a key point to control both reactivity and product selectivity of the catalyst is the nature of the ligand framework around the Lewis acidic metal centre. In this context, our research group has extensively studied the coordination chemistry of novel heteroscorpionate ligands [46], and a wide variety of applications have been reported in homogenous catalysis. For instance, we have designed versatile NNO-scorpionate alkyl and acetate zinc complexes that behaved as single-component initiators for the ring-opening co- and polymerization of cyclic esters [47-50], and for the ring-opening copolymerization of cyclohexene oxide with CO_2 [51], respectively, as well as dinuclear NNO-scorpionate alkyl zinc analogues that displayed excellent performances in the cycloaddition of epoxide with carbon dioxide under mild and solvent-free conditions [52].Now, we take on the challenge of designing more efficient cooperative homodinuclear NNO-scorpionate zinc catalysts containing thioalkoxide auxiliary ligands to enhance catalytic activity for CO2 fixation into the selective production of polycarbonates under milder conditions.

Hereby, we report the design of multinuclear scorpionate organo-zinc complexes and their use as efficient catalysts for the ring-opening copolymerization of cyclohexene oxide and carbon dioxide to produce poly(cyclohexene carbonate) under mild conditions.

Previous work

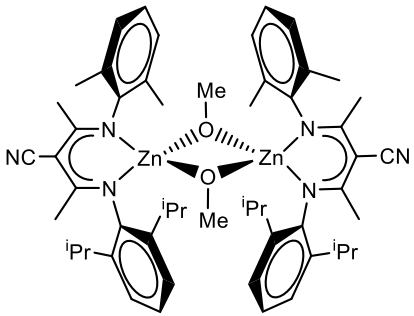

TOF = 2,290 h^{-1}, PCHC Select. = 90 %
50 °C, 6.9 bar CO_2
Angew. Chem. Int. Ed. **2002** [25]

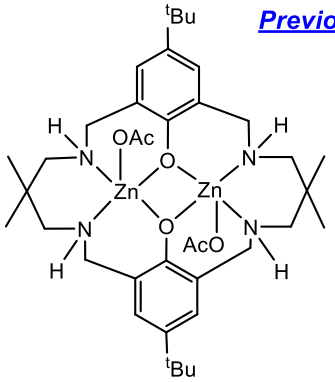

TOF = 140 h^{-1}, PCHC Select. = 95 %
100 °C, 10 bar CO_2
Angew. Chem. Int. Ed. **2009** [24]

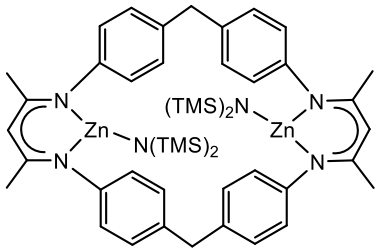

TOF = 5,900 h^{-1}, PCHC Select. = 99 %
100 °C, 30 bar CO_2
Chem. Eur. J. **2015** [23]

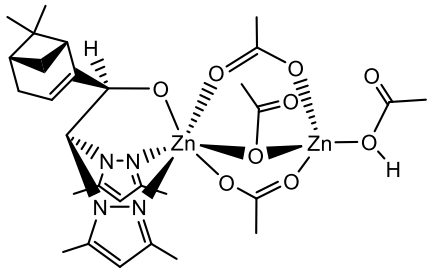

TOF = 5.6 h^{-1}, PCHC Select. = 90 %
80 °C, 40 bar CO_2
Polym. Chem. **2016** [51]

This work

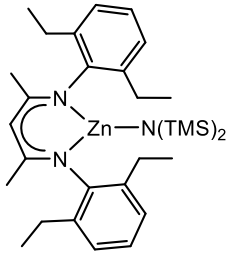

TOF = 5,520 h^{-1}, PCHC Select. = 93 %
50 °C, 40 bar CO_2
Chem. Sci. **2017** [18]

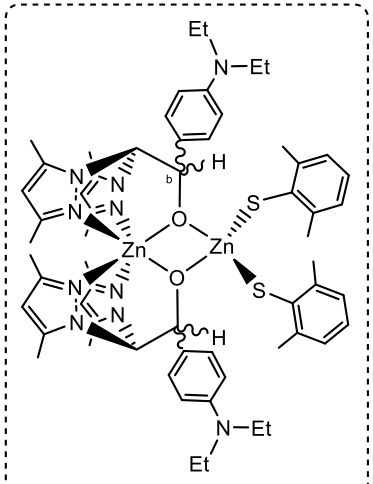

TOF = 4.3 h^{-1}, PCHC Select. = 95 %
70 °C, 10 bar CO_2

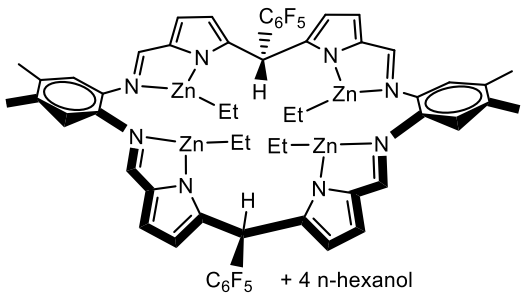

TOF = 21 h^{-1}, PCHC Select. = 56 %
80 °C, 30 bar CO_2
Dalton Trans. **2019** [17]

Chart 1. Representative zinc-based catalysts for the synthesis of poly(cyclohexene carbonate) via ROCOP of cyclohexene oxide and CO_2.

2. Materials and Methods

2.1. Materials

All manipulations were carried out under a nitrogen atmosphere using standard Schlenk techniques or a glovebox. Solvents were predried over sodium wire and distilled under nitrogen from sodium (toluene and *n*-hexane) or sodium-benzophenone (THF and diethyl ether). Deuterated solvents were stored over activated 4 Å molecular sieves and degassed by several freeze-thaw cycles. The zinc alkyls ZnR_2 (R = Me, Et) and 2,6-dimethylphenol or 2,6-dimethylthiophenol were used as purchased (Aldrich). The starting materials bpzampeH [53], and bpzaepeH [53] were also prepared according to literature procedures.

2.2 Experimental

2.2.1. Nuclear Magnetic Resonance Spectroscopy (NMR)

NMR spectra were recorded on Bruker Advance Neo 500 (^{1}H NMR 500 MHz and ^{13}C NMR 125 MHz) spectrometer and referenced to the residual deuterated solvent. The NOESY-1D spectra were recorded with the following acquisition parameters: irradiation time 2 s and number of scans 256, using standard VARIAN-FT software. Two-dimensional NMR spectra were acquired using standard VARIAN-FT software and processed using an IPC-Sun computer.

2.2.2. Elemental Analysis

Microanalyses were performed with a Perkin-Elmer 2400 CHN analyzer.

2.2.3. Gel Permeation Chromatography (GPC)

The molecular weights (M_n) and the molecular mass distributions (M_w/M_n) of polymer samples were measured by Gel Permeation Chromatography (GPC) performed on a Shimadzu LC-20AD GPC equipped with a TSK-GEL G3000Hxl column and an ELSD-LTII light-scattering detector. The GPC column was eluted with THF at 40 °C at 1 mL/min and was calibrated using eight monodisperse polystyrene standards in the range 580–483 000 Da. MALDI-ToF MS spectra were acquired with a Bruker Autoflex II ToF/ToF spectrometer, using a nitrogen laser source (337 nm, 3 ns) in linear mode with a positive acceleration voltage of 20 kV. Samples were prepared as follows: PC (2 mg) was dissolved in HPLC quality THF with dithranol as matrix and NaOAc as cationization agent in a 100:5:5 ratios. Before evaporation, 10 µL of the mixture solution was deposited on the sample plate. External calibration was performed by using Peptide Calibration Standard II (covered mass range: 700–3 200 Da) and Protein Calibration Standard I (covered mass range: 5 000–17 500 Da).

2.2.4. Crystallographic Refinement and Structure Solution

Crystals suitable for X-ray diffraction were obtained for **4**, **5** and **6**. The crystals were selected under oil and attached to the tip of a nylon loop. The crystals were mounted in a stream of cold nitrogen at 240-250 K for **4** and **6** and centred in the X-ray beam.

The crystal evaluation and data collection were performed on a Bruker X8 APEX II CCD-based diffractometer with MoKα (λ= 0.71073 Å) radiation. The initial cell constants were obtained from three series of scans at different starting angles. The reflections were successfully indexed by an automated indexing routine built in the SAINT program [54]. The absorption correction was based on fitting a function to the empirical transmission surface as sampled by multiple equivalent measurements [55]. A successful solution by the direct methods [56,57] provided most non-hydrogen atoms from the E-map. The remaining non-hydrogen atoms were located in an alternating series of

least-squares cycles and difference Fourier maps. All non-hydrogen atoms were refined with anisotropic displacement coefficients. All hydrogen atoms were included in the structure factor calculation at idealized positions and were allowed to ride on the neighboring atoms with relative isotropic displacement coefficients. Compounds **4** and **5** show some disordered molecules of THF solvent and we have considered appropriate squeeze them [58].

Final R(F), wR(F2) and goodness-of-fit agreement factors, details on the data collection and analysis can be found in Table S1.

2.3 General Procedures

2.3.1. Preparation of Compounds 1−6

Synthesis of [Zn(2,6-$Me_2C_6H_3O$)(bpzampe)]$_2$ 1. In a 250 cm^3 Schlenk tube, [Zn(Me)(bpzampe)] [29] (1.0 g, 2.31 mmol) was dissolved in dry toluene (60 mL) and the solution was cooled to 0 °C. A solution of 2,6-dimethylphenol (0.28 g, 2.31 mmol) in toluene was added and the mixture was allowed to warm up to room temperature and stirred during 1 h. The solvent was evaporated to dryness under reduced pressure to yield a white product. The product was washed with *n*-hexane (1 × 25 mL) to give compound **1** as a white solid. Yield: (1.12 g, 90%) Anal. Calcd. For $C_{56}H_{70}N_{10}O_4Zn_2$: C, 62.39; H, 6.55; N, 12.99. Found: C, 62.08; H, 6.58; N, 13.14. ^{1}H NMR (C_6D_6, 297 K), δ 7.15 (d, $^3J_{H\text{-}H}$ = 7.5 Hz, 4H, N-Ph^o), 6.98 (bs, 4H, *m*-H-OAr), 6.83 (t, $^3J_{H\text{-}H}$ = 7.1 Hz, 2H, *p*-H-OAr), 6.41 (d, $^3J_{H\text{-}H}$ = 7.5 Hz, 4H, N-Ph^m), 5.53 (s, 2H, CH^b), 5.48 (s, 2H, CH^a), 5.31, 5.10 (s, 4H, H$^{4,4'}$), 2.42 (bs, 12H, $(CH_3)_2$-OAr), 2.38 (s, 12H, -N-($\underline{CH_3}$)$_2$), 2.28 (s, 6H, Me^3), 2.18 (s, 6H, Me$^{3'}$), 1.79 (s, 6H, Me$^{5'}$), 1.11 (s, 6H, Me^5). ^{13}C {^{1}H} NMR (C_6D_6, 297 K), δ 161.6 (*ipso*-C-OAr), 159.0-153.0 (C$^{3,3'}$, C$^{5,5'}$), 132.0 (N-Ph^o), 128.6 (*o*-C-OAr), 127.3 (*m*-C-OAr), 124.1 (*p*-C-OAr), 111.5 (N-Ph^m), 102.2 (C$^{4'}$), 101.0 (C^4), 74.9 (C^a), 72.1 (C^b), 39.8 ($\underline{Me_2}$-OAr), 25.1 (N-CH_3), 13.5, 13.3 (Me$^{3,3'}$), 10.2, 9.9 (Me$^{5,5'}$).

Synthesis of [Zn(2,6-$Me_2C_6H_3O$)(bpzaepe)]$_2$ 2. The synthesis of **2** was carried out in an identical manner to **1**, using **[Zn(Me)(bpzaepe)]** (1.0 g, 2.17 mmol) and 2,6-dimethylphenol (0.26 g, 2.17 mmol), to give **2** as a white solid. Yield: (1.17 g, 91%). Anal. Calcd. For $C_{60}H_{78}N_{10}O_4Zn_2$: C, 63.54; H, 6.93; N, 12.35. Found: C, 63.59; H, 6.98; N, 12.43. ^{1}H NMR (C_6D_6, 297 K), δ 7.17 (d, $^3J_{H\text{-}H}$ = 7.5 Hz, 4H, N-Ph^o), 7.04 (bs, 4H, *m*-H-OAr), 6.75 (t, $^3J_{H\text{-}H}$ = 7.1 Hz, 2H, *p*-H-OAr), 6.59 (d, $^3J_{H\text{-}H}$= 7.5 Hz, 4H, N-Ph^m), 5.51 (s, 2H, CH^b), 5.43 (s, 2H, CH^a), 5.42, 5.18 (s, 4H, H$^{4,4'}$), 2.95 (m, 8H, N-$\underline{CH_2}CH_3$), 2.63, 2.30 (bs, 12H, $(CH_3)_2$-OAr), 2.16 (s, 6H, Me^3), 1.97 (s, 6H, Me$^{3'}$), 1.72 (s, 6H, Me$^{5'}$), 1.12 (s, 6H, Me^5), 0.89 (t, $^3J_{H\text{-}H}$ = 8.0 Hz, 12H, N-$CH_2\underline{CH_3}$). ^{13}C {^{1}H} NMR (C_6D_6, 297 K), δ 158.1 (*ipso*-C-OAr), 156.5-153.9 (C$^{3,3'}$, C$^{5,5'}$), 132.0 (N-Ph^o), 128.4 (*o*-C-OAr), 127.9 (*m*-C-OAr), 124.2 (*p*-C-OAr), 111.5 (N-Ph^m), 102.3 (C$^{4'}$), 101.1 (C^4), 76.9 (C^a), 71.4 (C^b), 39.9 ($\underline{Me_2}$-OAr), 39.1 (N-$\underline{CH_2}CH_3$), 13.4, 13.3 (Me$^{3,3'}$), 12.1 (N-$CH_2\underline{CH_3}$), 10.2, 9.8 (Me$^{5,5'}$).

Synthesis of [Zn(bpzampe)$_2${Zn(2,6-$Me_2C_6H_3S$)$_2$}] 3. The synthesis of **3** was carried out in an identical manner to **1**, using **[Zn(Me)(bpzampe)]** (1.0 g, 2.31 mmol) and 2,6-dimethylthiophenol (0.31 mL, 2.31 mmol) to give **3** as a pale yellow solid. Yield: (1.21 g, 95%). Anal. Calcd. For $C_{56}H_{70}N_{10}O_2S_2Zn_2$: C, 60.59; H, 6.36; N, 12.62. Found: C, 60.63; H, 6.40; N, 12.55. ^{1}H NMR (C_6D_6, 297 K): δ 7.78 (d, $^3J_{H\text{-}H}$ = 7.5 Hz, 4H, N-Ph^o), 6.95 (bs, 4H, *m*-H-SAr), 6.81 (t, $^3J_{H\text{-}H}$ = 7.1 Hz, 2H, *p*-H-SAr), 6.81 (d, $^3J_{H\text{-}H}$ = 7.5 Hz, 4H, N-Ph^m), 6.21 (s, 2H, CH^b), 6.10 (s, 2H, CH^a) 5.78, 5.26 (s, 4H, H$^{4,4'}$), 2.62 (s, 12H, -N-($\underline{CH_3}$)$_2$), 2.58 (bs, 12H, $(CH_3)_2$-SAr), 2.33 (s, 6H, Me^3), 1.81 (s, 6H, Me$^{3'}$), 1.63 (s, 6H, Me$^{5'}$), 1.49 (s, 6H, Me^5). ^{13}C {^{1}H} NMR (C_6D_6, 297 K), δ 158.3 (*ipso*-C-SAr), 142.5-138.0 (C$^{3,3'}$, C$^{5,5'}$), 128.9 (N-Ph^o), 128.6 (*o*-C-SAr), 128.3 (*m*-C-SAr), 127.5 (*p*-C-SAr), 111.8 (N-Ph^m), 106.6 (C$^{4'}$), 106.5 (C^4), 77.6 (C^a), 70.0 (C^b), 24.5 ($\underline{Me_2}$-SAr), 19.8 (N-CH_3), 13.8, 13.7 (Me$^{3,3'}$), 10.2, 10.1 (Me$^{5,5'}$).

Synthesis of [Zn(bpzaepe)$_2${Zn(2,6-Me$_2$C$_6$H$_3$S)$_2$}] 4. The synthesis of **4** was carried out in an identical manner to **1**, using **[Zn(Me)(bpzaepe)]** (1.0 g, 2.17 mmol) and 2,6-dimethylthiophenol (0.29 mL, 2.17 mmol), to give **4** as a pale yellow solid. This complex was crystallized in 20 mL of THF and crystals sustainable for X ray diffraction analysis were obtained. Yield: (1.22 g, 97%). Anal. Calcd. For $C_{60}H_{78}N_{10}O_2S_2Zn_2$: C, 61.79; H, 6.74; N, 12.01. Found: C, 61.89; H, 6.63; N, 12.00. ^{1}H NMR ($CDCl_3$, 297 K): δ 7.77 (d, $^3J_{H\text{-}H}$= 7.5 Hz, 4H, N-Ph^o), 6.98 (bs, 4H, *m*-H-SAr), 6.82 (t, $^3J_{H\text{-}H}$ = 7.1 Hz, 2H, *p*-H-SAr), 6.81 (d, $^3J_{H\text{-}H}$ = 7.5 Hz, 4H, N-Ph^m), 6.21 (s, 2H, CH^b), 6.11 (s, 2H, CH^a) 5.79, 5.25 (s, 4H, H$^{4,4'}$), 3.10 (m, 8H, N-$\underline{CH_2}CH_3$), 2.58 (bs, 12H, $(CH_3)_2$-SAr), 2.15, 1.82 (s, 12H, Me$^{3,3'}$), 1.63 (s, 6H, Me$^{5'}$), 1.50 (s, 6H, Me^5), 1.00 (t, $^3J_{H\text{-}H}$ = 8.0 Hz, 12H, N-$CH_2\underline{CH_3}$). ^{13}C {^{1}H} NMR (C_6D_6, 297 K), δ 159.1 (*ipso*-C-SAr), 142.2-138.1 (C$^{3,3'}$, C$^{5,5'}$), 129.3 (N-Ph^o), 128.6 (*o*-C-SAr), 128.3 (*m*-C-SAr), 126.3 (*p*-C-SAr), 111.9 (N-Ph^m), 107.3 (C$^{4'}$), 107.2 (C^4), 78.0 (C^a), 70.1 (C^b), 44.0 (N-$\underline{CH_2}CH_3$), 24.6 ($\underline{Me_2}$-SAr), 13.7, 13.6 (Me$^{3,3'}$), 12.5 (N-$CH_2\underline{CH_3}$), 10.2, 10.1 (Me$^{5,5'}$).

Synthesis of [Zn(2,6-Me$_2$C$_6$H$_3$S)$_2$(Hbpzampe)] 5. The synthesis of **5** was carried out in an identical manner to **3**, but using two equivalents of 2,6-dimethylthiophenol (0.62 mL, 4.62 mmol), to give **5** as a pale yellow solid. This complex was crystallized in 20 mL of THF and crystals sustainable for X ray diffraction analysis were obtained. Yield: (1.50 g, 94%). Anal. Calcd. For $C_{36}H_{45}N_5OS_2Zn$: C, 62.37; H, 6.54; N, 10.10. Found: C, 62.47; H, 6.56; N, 10.21. ^{1}H NMR ($CDCl_3$, 297 K): δ 6.98 (d, $^3J_{H\text{-}H}$ = 7.5 Hz, 2H, N-Ph^o), 6.92 (bs, 2H, *m*-H-SAr), 6.83 (t, $^3J_{H\text{-}H}$ = 7.1 Hz, 1H, *p*-H-SAr), 6.39 (d, $^3J_{H\text{-}H}$= 7.5 Hz, 2H, N-Ph^m), 5.61 (s, 1H, CH^b), 5.51 (s, 1H, CH^a), 5.40, 5.10 (s, 2H, H$^{4,4'}$), 3.01 (s, 6H, -N-($\underline{CH_3}$)$_2$), 2.41, 2.34 (bs, 12H, $(CH_3)_2$-SAr), 2.25 (s, 3H, Me^3), 2.18 (s, 3H, Me$^{3'}$), 1.83 (s, 3H, Me$^{5'}$), 1.18 (s, 3H, Me^5). ^{13}C {^{1}H} NMR (C_6D_6, 297 K), δ 160.3 (*ipso*-C-SAr), 152.3-141.1 (C$^{3,3'}$, C$^{5,5'}$), 129.8 (N-Ph^o), 129.6 (*o*-C-SAr), 128.3 (*m*-C-SAr), 122.5 (*p*-C-SAr), 111.9 (N-Ph^m), 107.2 (C$^{4'}$), 106.3 (C^4), 78.3 (C^a), 68.6 (C^b), 24.1, 22.2 ($\underline{Me_2}$-SAr), 19.6 (N-CH_3), 13.9, 13.8 (Me$^{3,3'}$), 10.2, 9.9 (Me$^{5,5'}$).

Synthesis of [Zn(2,6-Me$_2$C$_6$H$_3$S)$_2$(Hbpzaepe)] 6. The synthesis of **6** was carried out in an identical manner to **4**, but using two equivalents of 2,6-dimethylthiophenol (0.58 mL, 4.34 mmol) to give **6** as a pale yellow solid. This complex was crystallized in 20 mL of THF and crystals sustainable for X ray diffraction analysis were obtained. Yield: (1.44 g, 92%). Anal. Calcd. For $C_{38}H_{49}N_5OS_2Zn$: C, 63.27; H, 6.85; N, 9.71. Found: C, 63.40; H, 6.72; N, 10.03. ^{1}H NMR (C_6D_6, 297 K), δ 6.97 (d, $^3J_{H\text{-}H}$ = 7.5 Hz, 2H, N-Ph^o), 6.95 (bs, 2H, *m*-H-SAr), 6.85 (t, $^3J_{H\text{-}H}$ = 7.1 Hz, 1H, *p*-H-SAr), 6.37 (d, $^3J_{H\text{-}H}$ = 7.5 Hz, 2H, N-Ph^m), 5.58 (s, 1H, CH^b), 5.45 (s, 1H, CH^a) 5.39, 5.10 (s, 2H, H$^{4,4'}$), 2.84 (m, 4H, N-$\underline{CH_2}CH_3$), 3.00, 2.33 (bs, 12H, $(CH_3)_2$-SAr), 2.30, 2.19 (s, 6H, Me$^{3,3'}$), 1.91 (s, 3H, Me$^{5'}$), 1.18 (s, 3H, Me^5), 0.83 (t, 6H, $^3J_{H\text{-}H}$ = 8.0 Hz, N-$CH_2\underline{CH_3}$). ^{13}C {^{1}H} NMR (C_6D_6, 297 K), δ 160.3 (*ipso*-C-SAr), 152.3-141.4 (C$^{3,3'}$, C$^{5,5'}$), 129.9 (N-Ph^o), 128.6 (*o*-C-SAr), 128.3 (*m*-C-SAr), 122.5 (*p*-C-SAr), 111.8 (N-Ph^m), 107.2 (C$^{4'}$), 106.3 (C^4), 78.2 (C^a), 68.4 (C^b), 44.0 (N-$\underline{CH_2}CH_3$), 24.1, 22.5 ($\underline{Me_2}$-SAr), 13.9, 13.8 (Me$^{3,3'}$), 12.1 (N-$CH_2\underline{CH_3}$), 10.1, 9.9 (Me$^{5,5'}$), 10.0 (N-$CH_2\underline{CH_3}$).

2.3.2. General Procedure for the Synthesis of Polycarbonates

Cyclohexene oxide (0.98 g, 10.0 mmol) and catalysts **2**, **4** and **6** (0.1 mmol) were placed in a stainless steel reactor with a magnetic stirrer bar. The autoclave was sealed, pressurized to 5 bar with CO_2, heated to the desired temperature and then pressurized to 1–40 bar with CO_2. The reaction mixture was subsequently stirred at 50–100 °C for 2–16 h. The conversion of cyclohexene oxide into poly(cyclohexene carbonate) was determined by analysis of a sample by ^{1}H NMR spectroscopy. Poly(cyclohexene carbonate) is a known compound and the spectroscopic data of samples prepared using catalysts **2**, **4** and **6** were consistent with those reported in the literature.

3. Results

3.1. Synthesis and Characterization of Complexes

We have explored additional aspects concerning to the reactivity of the previously described in our group mononuclear chiral complexes [Zn(Me)(κ^3-NNO)] [53] [κ^3-NNO = bpzampe = {2,2-bis(3,5-dimethylpyrazol-1-yl)-1-[4-(dimethylamino)phenyl]ethoxide} or bpzaepe = {2,2-bis(3,5-dimethylpyrazol-1-yl)-1-[4-(diethylamino)phenyl]ethoxide}], with several aromatic alcohols or thioalcohols, and new complexes that contain aryloxide or thioaryloxide ligands were isolated after methane elimination. Thus, the alcoholysis or thioalcoholysis reaction of these monoalkyl complexes with ArEH (Ar = 2,6-$Me_2C_6H_3$; E = O, S), in a 1:1 molar ratio, yields the chiral dinuclear zinc complexes [Zn(OAr)(κ^2-NNμ-O)]$_2$ **1**–**2** (κ^2-NNμ-O = bpzampe **1**, bpzaepe **2**) and [Zn(κ^2-NN-μ-O)$_2${Zn(SAr)$_2$}] **3**–**4** (κ^2-NNμ-O = bpzampe **3**, bpzaepe **4**), whereas when this reaction was carried out in a 1:2 molar ratio of thioalcohol, the mononuclear compounds [Zn(SAr)$_2$(κ^2-NN-OH)] **5**–**6** (κ^2-NN-OH = Hbpzampe **5**, Hbpzaepe **6**) were obtained (see Scheme 2). The analogous reaction (1:2 molar ratio) with the alcohol led to dinuclear complexes **1**–**2**.

The different complexes were characterized spectroscopically (see Figures S1-S3). The ^{1}H and ^{13}C{^{1}H} NMR spectra of **1**–**6** exhibit two distinct sets of pyrazole resonances, which indicate the existence of two types of pyrazole rings. The ^{1}H NMR spectra of these complexes show two singlets for each of the H^4, Me^3 and Me^5 pyrazole protons, one broad singlet for each of the methine groups (the bridging CH^a group to the two pyrazole rings and the sterogenic CH^b), and the signals corresponding to the R' moieties of the scorpionate ligands as well as the alkyl, aryloxide or thioaryloxide ligands.

These results are consistent with a geometric environment for the zinc atoms in which the two pyrazole rings are located in *cis* and *trans* positions with respect to the 4-(dimethylamino)phenyl or 4-(diethylamino)phenyl groups (see Scheme 2). The ^{1}H NOESY-1D experiments enabled the unequivocal assignment of all ^{1}H resonances, and the assignment of the ^{13}C {^{1}H}-NMR signals was carried out on the basis of ^{1}H-^{13}C heteronuclear correlation (g-HSQC) experiments. In addition, in the dinuclear complexes **1**–**4**, the fact that only two sets of signals are observed for the pyrazole resonances indicates that only one diastereoisomer was present in solution of the two possible (*meso* and *rac*).

The dimeric structure proposed for complexes **1** and **2** (see Scheme 2) is in good agreement with the NMR experiments. The heteroscorpionate ligand is attached to the zinc centre through the nitrogen atoms from both pyrazole rings, and the oxygen atom from the alkoxide moiety bridges the two zinc centres in a κ^2-NNμ-O coordination mode. In addition, each zinc atom is coordinated to an aryloxide ligand. The geometry around each zinc metal is a distorted square planar pyramid. This proposed structure is similar to that found for the compound [Zn(OAr)(bpzte)]$_2$ (bpzte = 2,2-bis(3,5-dimethylpyrazol-1-yl)-1-para-tolylethoxide], previously reported [48], which was obtained by an analogous reaction. In that complex, X-ray diffraction analysis confirmed this geometrical disposition, with a rhomboidal $(ZnO)_2$ core similar to that proposed for complexes **1** and **2**.

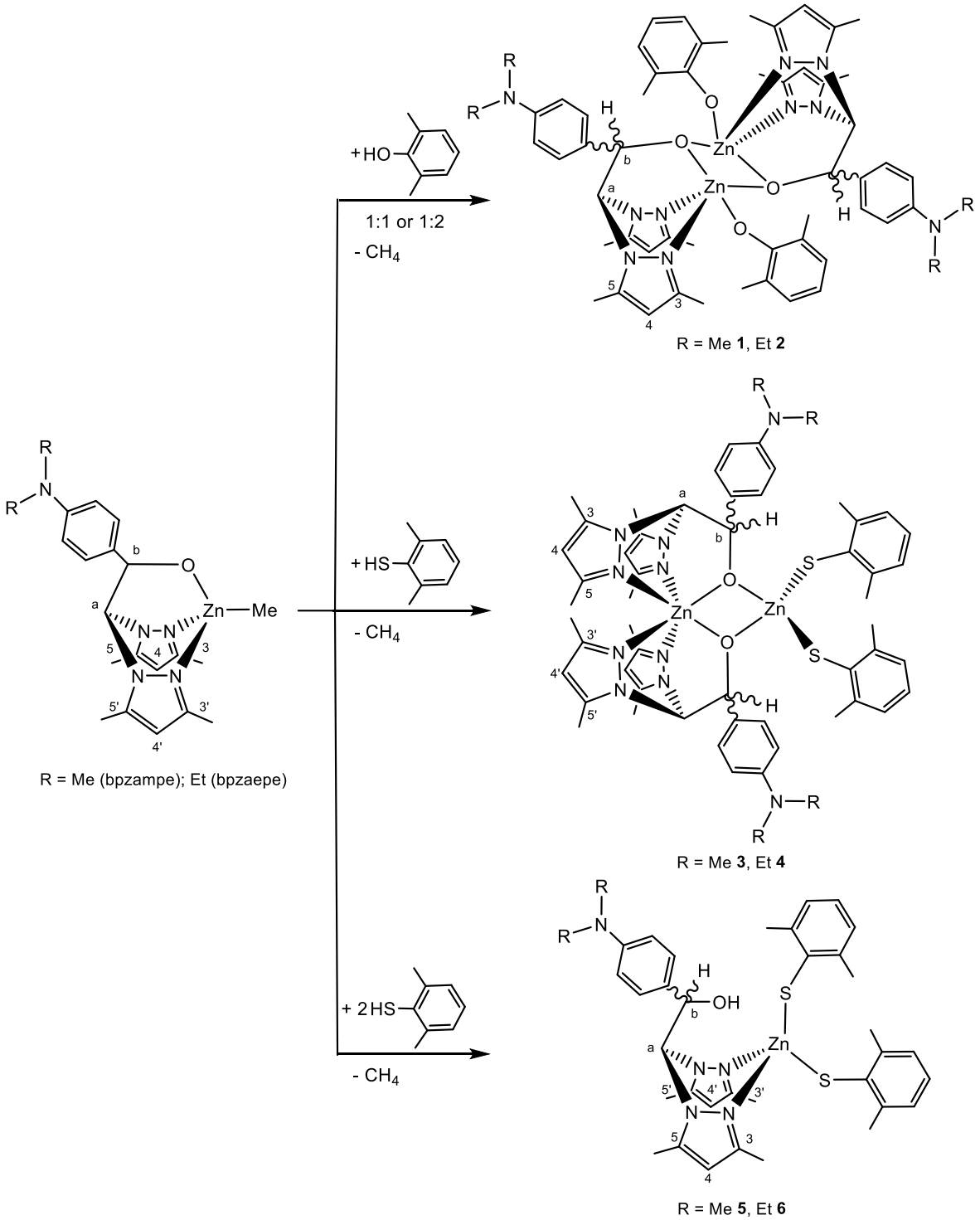

Scheme 2. Synthesis of NNO-scorpionate aryloxide and thioaryloxide zinc complexes **1**–**6**.

An X-ray crystal structure determination was carried out for **4**. The ORTEP drawing is shown in Figure 1. A summary of bond lengths and angles is presented in Table 1 and the crystallographic details are reported in Table S1. Only one diastereoisomer, namely "rac", was present in the unit cell. These studies confirmed that the presence in solution of only one diastereoisomer for these compounds is maintained in the solid-state. The complexes have a dinuclear structure with two μ-bridging alkoxide groups from the scorpionate ligands between the two six- and four-coordinate Zn(II) atoms. The first zinc centre Zn(1) has a distorted octahedral geometry with a heteroscorpionate ligand that acts in a tridentate fashion. The pyrazolic nitrogens N(1), N(3), N(6) and N(8) occupy four positions and the alkoxide oxygen-bridging μ-O(1) and μ-O(2) occupy the other two positions. The

second zinc centre Zn(2) has a distorted tetrahedral geometry in which μ-O(1) and μ-O(2) occupy two positions, and the thioaryloxide groups the other two positions [Zn(2)–S distances = 2.287(3) and 2.277(3)]. Furthermore, the X-ray structure of **4** has a rhomboidal $(ZnO)_2$ core with Zn(1)–O(1), Zn(1)–O(2), Zn(2)–O(1) and Zn(2)–O(2) bond lengths ranging from 2.032(5) to 2.048(5) Å and the Zn···Zn diagonal 2.974(1) Å is much longer than the O···O diagonal 2.793(5) Å. The dimeric aggregate is based on Zn_2O_2 four-membered rings, which have previously been observed in other zinc compounds that contain, for example, thiolate-oxo, alkoxide-imino, aryloxide or aminoalcoholate ligands [59-62], and, more recently, by our research group with dinuclear complexes of the type [Zn(R)(κ-NNμ-O)]$_2$ [48]. However, it should be noted that only one dinuclear compound of zinc with two six- and four-coordinate Zn(II) atoms, based on Zn_2O_2 four-membered rings, containing a scorpionate ligand have been reported in the literature [50].

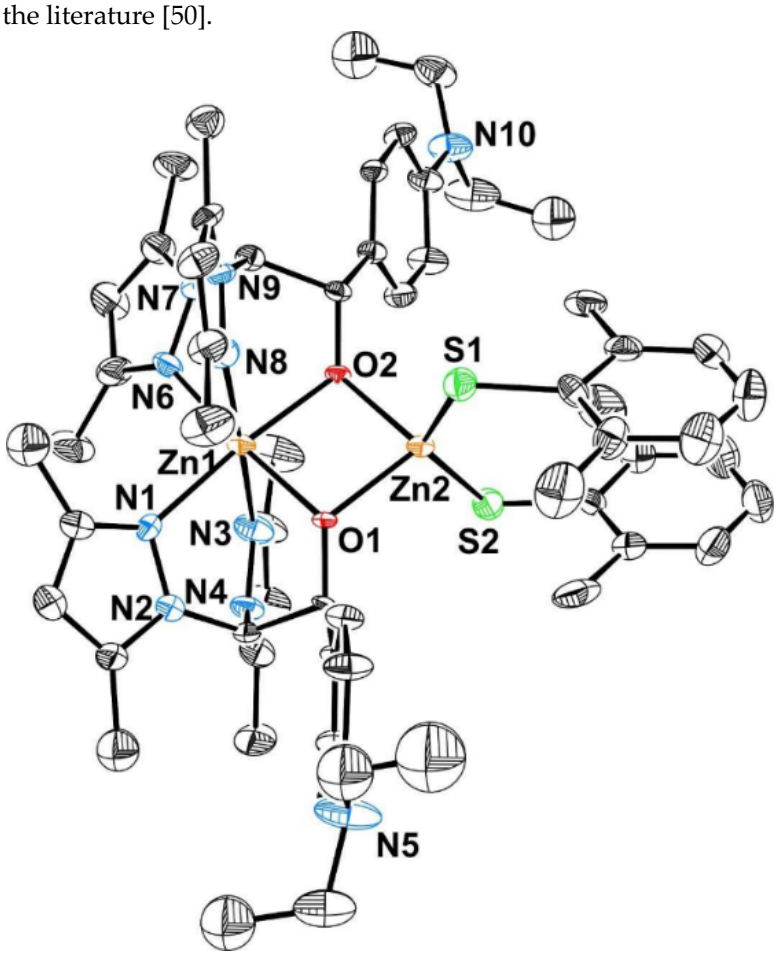

Figure 1. ORTEP view of the *S,S* enantiomer of [Zn(bpzaepe)$_2${Zn(2,6-Me$_2$C$_6$H$_3$S)$_2$}] (**4**). Hydrogen atoms have been omitted for clarity. Thermal ellipsoids are drawn at the 30% probability level.

Complexes **5** and **6** were also characterized by single-crystal X-ray diffraction and the molecular structures are shown in Figure 2 and the Figure S4, respectively. This study confirmed that the presence in solution of the corresponding two enantiomers (R + S) is maintained in the solid state. The most representative bond lengths and angles, and crystallographic details are presented in Table 1 and Table S1, respectively. These complexes have a monomeric structure that consists of a heteroscorpionate ligand bonded to the zinc atom through the two nitrogen atoms in a κ^2-NN-coordination mode. In addition, the zinc centre is coordinated to two thioaryloxide ligands. This centre has a distorted tetrahedral environment due to the κ^2-NN-coordination of the scorpionate ligand with major distortion in the N(1)–Zn(1)–N(3) angle, which has a value of 91.6(2)° for complex **5**. The Zn–N distances [2.047(5) Å and 2.067(5) Å] for Zn(1)–N(1) and Zn(1)–N(3) in complex **5**, are in good agreement with other values determined for zinc scorpionate complexes such as [Zn(CH$_3$)(bpzbe)] [63] or [Zn(CH$_3$)(pbp^{t}amd)] [64] prepared by our research group. Finally, the Zn–S distances [2.290(2) Å and 2.265(2) Å] for **5** are similar to those found for complex **4**.

Table 1. Selected bond lengths (Å) and angles (º) for **4**, **5** and **6**

Bond Lengths					
4		**5**		**6**	
N(1)-Zn(1)	2.133(7)	Zn(1)-N(1)	2.047(5)	Zn(1)-N(1)	2.047(3)
N(3)-Zn(1)	2.230(7)	Zn(1)-N(3)	2.067(5)	Zn(1)-N(3)	2.082(3)
N(6)-Zn(1)	2.117(7)	Zn(1)-S(2)	2.265(2)	Zn(1)-S(1)	2.268(1)
N(8)-Zn(1)	2.226(7)	Zn(1)-S(1)	2.290(2)	Zn(1)-S(2)	2.296(1)
O(1)-Zn(2)	2.032(5)	S(1)-C(29)	1.763(8)	S(1)-C(23)	1.769(5)
O(1)-Zn(1)	2.044(5)	S(2)-C(21)	1.765(7)	S(2)-C(31)	1.771(5)
O(2)-Zn(2)	2.036(4)	O(1)-C(12)	1.414(7)	O(1)-C(12)	1.414(4)
O(2)-Zn(1)	2.048(5)				
S(1)-Zn(2)	2.287(3)				
S(2)-Zn(2)	2.277(3)				
Zn(1)-Zn(2)	2.974(1)				
C(45)-S(1)	1.789(9)				
C(53)-S(2)	1.763(9)				
Angles					
S(2)-Zn(2)-S(1)	134.15(9)	S(2)-Zn(1)-S(1)	99.87(8)	S(1)-Zn(1)-S(2)	98.87(4)
O(1)-Zn(1)-O(2)	86.1(2)	N(1)-Zn(1)-N(3)	91.6(2)	N(1)-Zn(1)-N(3)	91.7(1)
N(6)-Zn(1)-N(1)	98.7(3)	N(1)-Zn(1)-S(1)	115.1(2)	N(1)-Zn(1)-S(1)	122.9(1)
N(8)-Zn(1)-N(3)	176.9(3)	N(3)-Zn(1)-S(2)	114.3(2)	N(3)-Zn(1)-S(2)	113.6(1)
O(1)-Zn(2)-O(2)	86.7(2)				

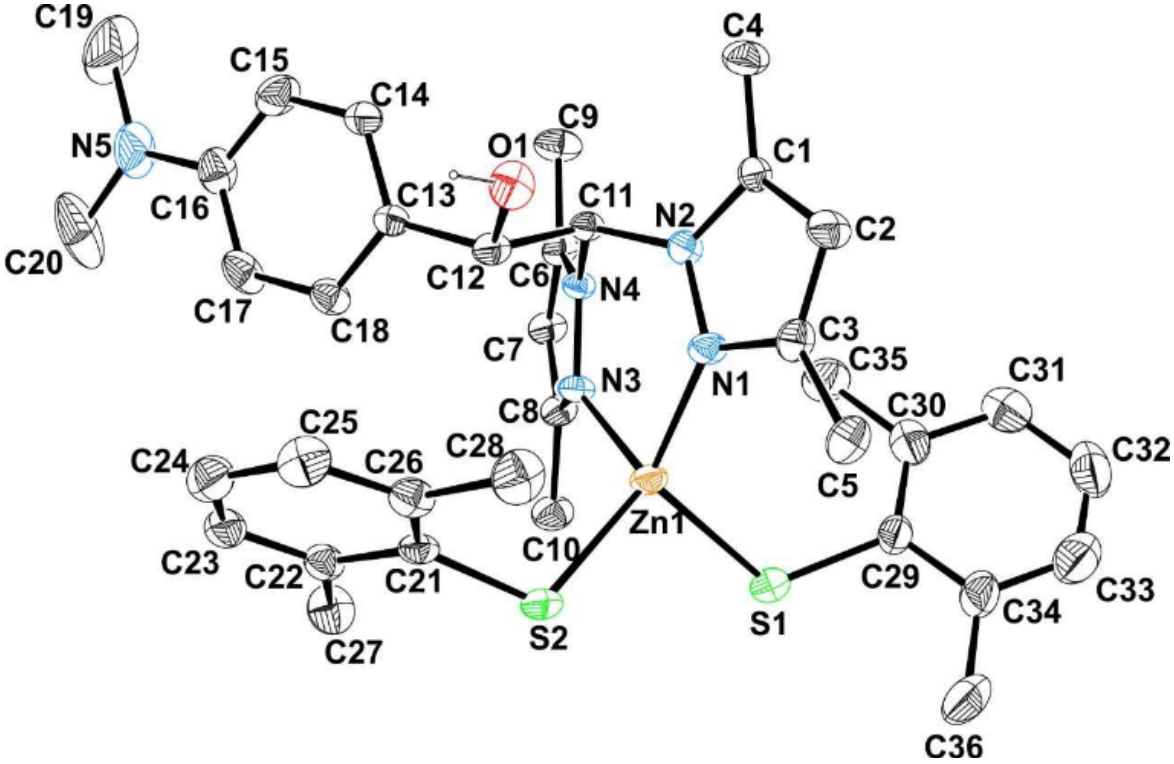

Figure 2. ORTEP view of the *S* enantiomer of [Zn(2,6-$Me_2C_6H_3S)_2$(Hbpzampe)] (**5**). Hydrogen atoms have been omitted for clarity. Thermal ellipsoids are drawn at the 30% probability level.

3.2. Catalytic Studies on the Ring-Opening Copolymerization of Cyclohexene Oxide with Carbon Dioxide

A representative complex of each type of molecular arrangement was selected for catalytic inspection. Thus, the dinuclear complexes **2** and **4**, and the mononuclear **6** were initially assessed for the conversion of cyclohexene oxide (CHO) into poly(cyclohexene carbonate (PCHC; **7**) at 80 °C and 40 bar of carbon dioxide pressure in the absence of a co-catalyst under solvent-free conditions for 16 hours, using 1 mol% of complexes **2**, **4** and **6** (see Scheme 3).

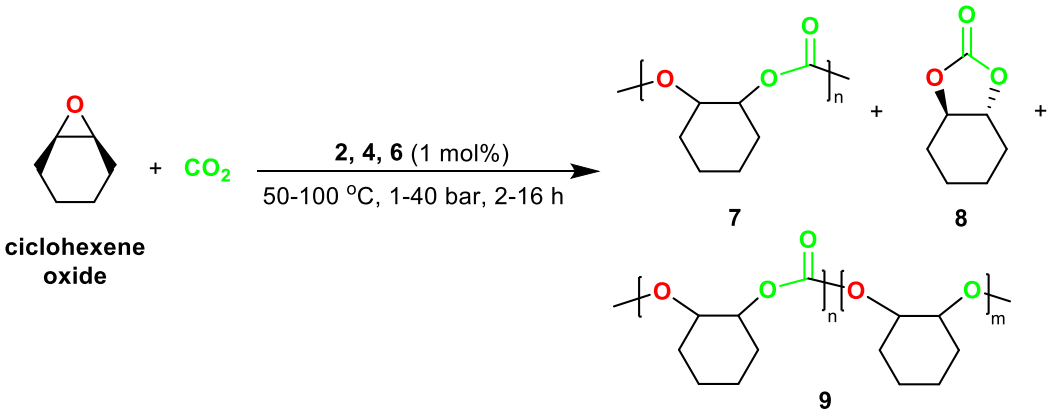

Scheme 3. Synthesis of poly(cyclohexene carbonate) catalysed by complexes **2**, **4** and **6**.

^{1}H NMR spectroscopy was employed to analyse each reaction without further purification and to determine the conversion of CHO into **7**, cyclohexene carbonate (CHC; **8**) or polyether–polycarbonate **9** (see Scheme 3). The results are presented on Table 2. Interestingly, complexes **2**, **4** and **6**, showed good to excellent conversions of cyclohexene oxide, in the absence of a co-catalyst, thus indicating that these complexes are able to initiate copolymerization by themselves [14].

In the case of the dinuclear thioalkoxide derivative **4**, the only polymeric species identified by ^{1}H NMR spectroscopy was poly(cyclohexene carbonate) **7**, in conjunction with *trans*-cyclohexene carbonate **8**, as a result of backbiting reactions (Table 2, entry 2). Contrarily, the mononuclear thioalkoxide complex **6** displayed lower selectivity for the formation of **7** (Table 2, entry 3) while the dinuclear alkoxide complex **2** showed a very low selectivity (Table 2, entry 1). Both complexes **2** and **6** presented higher selectivity for polyether polycarbonate **9** production than complex **4** (Table 2, entries 1–3). Thus, complex **4** exhibited the outperformed catalytic activity and carbonate selectivity for the ring-opening copolymerization of CHO and carbon dioxide (Table 2, entry 2), affording 75% conversion with a high content of carbonate linkages (>99%) and a very high PCHC/CHC ratio (93/7), possibly due to the presence of the hemilabile thioalkoxide ligand. Interestingly, very efficient and selective multinuclear zinc catalysts bearing different auxiliary ligands have been recently reported in the ROCOP of CHO and CO_2 (see Chart 1) [17,18,23-25,51]. However, as far as we are aware, no examples have been reported containing thioalkoxide auxiliary ligands [65].

Since complex **4** was more active and selective than **2** and **6** for the synthesis of **7**, complex **4** was finally selected for further optimization of the reaction. Thus, the effect of varying catalyst loading, the reaction temperature, reaction pressure and reaction time was inspected. The results are shown in Table S2 and Tables 3–5, respectively. Under the previous reaction conditions (80 °C, 40 bar of CO_2 pressure), the catalyst loading was finally optimized to 1 mol% (Table S2).

In addition, the catalytic activity of complex **4** was very dependent on the reaction temperature (Table 3). Thus, reduction of the temperature from 80 °C to 50 °C resulted in a dramatic decreasing on both conversion and selectivity of CHO to **7** (52% conv.; PCHC/CHC = 73/27) (Table 3, entry 1). In addition, decreasing in only 10 °C on the reaction temperature afforded a slight increase on the conversion of CHO into PCHC (79%), while led to a maintenance on selectivity to a PCHC/CHC ratio of 92/8. Conversely, the increasing of the reaction temperature up to 100 °C did not significantly increase the conversion of cyclohexene oxide into polymer **7**, but led to an important decrease in selectivity (PCHC/CHC = 72/28, Table 3, entries 3–5). Therefore, the optimized temperature for further experiments was 70 °C.

Table 2. Synthesis of poly(cyclohexene carbonate) catalysed by complexes **2**, **4** and **6**.[a]

Entry	Cat	Conv. (%)[b]	%CHC[b]	%Copolymer (%Carbonate linkage)[b]	TON[c]	TOF[d] (h^{-1})
1	**2**	52	44	56(64)	29	1.82
2	**4**	75	7	93 (>99)	70	4.36
3	**6**	65	15	85 (64)	55	3.45

[a] Reactions carried out at 80 °C and 40 bar CO_2 pressure for 16 hours using 1 mol% of catalyst. [b] Conversion, % of *trans*-CHC, % of PCHC and % of carbonate linkages determined by ^{1}H NMR spectroscopy of the crude reaction mixture. [c] TON = moles of PCHC/moles of catalyst. [d] TOF = TON/time (h).

Table 3. Effect of reaction temperature on the synthesis of poly(cyclohexene carbonate) catalysed by complex **4**[a]

Entry	Temp (°C)	Conv. (%)[b]	%CHC[b]	%Copolymer (%Carbonate linkage)[b]	TON[c]	TOF[d] (h^{-1})	$M_{n(exp)}$[e](M_w/M_n)[e]
1	50	52	27	73(>99)	38	2.37	5 100(1.33)
2	60	62	11	89(>99)	55	3.45	7 700(1.27)
3	70	79	8	92(>99)	73	4.54	10 700(1.03)
4	80	75	7	93 (>99)	70	4.36	10 100(1.07)
5	100	80	28	72 (>99)	58	3.60	8 500(1.15)

[a] Reactions carried out at 50–100 °C and 40 bar CO_2 pressure for 16 hours using 1 mol% of catalyst **4**. [b] Conversion, % of *trans*-CHC, % of PCHC and % of carbonate linkages determined by ^{1}H NMR spectroscopy of the crude reaction mixture. [c] TON = moles of product/moles of catalyst. [d] TOF = TON/time (h). [e] Determined by GPC relative to polystyrene standards in tetrahydrofuran.

The reaction pressure was also found to have a marked effect on the catalytic activity and selectivity, as presented on Table 4. Detrimental effect on conversion of complex **4** was observed when decreasing the reaction pressure from 40 to 1 bar (Table 4, entry 1). Interestingly, at 10 bar of CO_2 pressure, conversion and selectivity values were very similar to that found at 20 bar (72%, PCHC/CHC = 95/5), with the TOF 4.27 h^{-1}. Not expectedly, increasing of pressure at 30 bar did not produce a significant growth on the conversion value, while a lack of PCHC/CHC selectivity was observed (83/17). It was also noteworthy that the carbonate linkage (>99%) remained essentially constant in the range of 1 to 40 bar (Table 4, entries 1-5). Therefore, 10 bar was the optimized CO_2 pressure.

Finally, it was investigated the influence of reaction time on catalytic activity of complex **4**. As expected, at short periods of time (2 h), the conversion decreased from 72% to 17% (Table 5, entries 1-6), with a slight decreased of polymer selectivity (95% to 84%). Importantly, increase of the reaction time produced PCHC with higher molecular weights, with low dispersity values ranging from 1.33-1.05 (see Figure S5), suggesting the absence of back-biting reactions and that the ROCOP of cyclohexene oxide and CO_2 exhibits living propagations (see Figure 3).

Although the activity values found for complex **4** are considerably lower than that reported for alternative very efficient zinc complexes [18,23,24,25], the reaction conditions optimized for **4** are significantly milder than that described for some of these catalysts, and analogous previously reported scorpionate zinc complexes [51], showing a high level of PCHC selectivity (see Chart 1). In addition, pseudo-first order with respect to cyclohexene oxide consumption was confirmed from the semi-logarithmic plot of ln[CHO] versus reaction time, which displays a linear increase in monomer conversion with reaction time (see Figure S6).

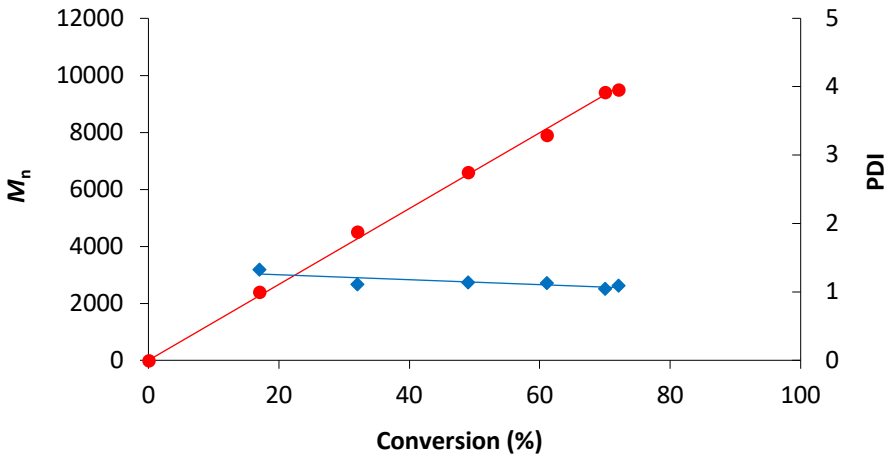

Figure 3. Plot of M_n versus CHO conversion (●) and M_w/M_n versus CHO conversion (♦) for compound **4** at 70 °C and 10 bar CO_2.

Table 4. Effect of reaction pressure on the synthesis of poly(cyclohexene carbonate) catalysed by complex **4**[a]

Entry	Pres. (bar)	Conv. (%)[b]	%CHC[b]	%Copolymer (%Carbonate linkage)[b]	TON[c]	TOF[d] (h^{-1})	$M_{n(exp)}$[e](M_w/M_n)[e]
1	1	55	10	90(>99)	50	3.09	7 400(1.13)
2	10	72	5	95(>99)	68	4.27	9 500(1.09)
3	20	70	3	97(>99)	68	4.24	9 800(1.03)
4	30	83	17	83(>99)	69	4.30	10 000(1.07)
5	40	79	8	92(>99)	73	4.54	10 700(1.03)

[a] Reactions carried out at 70 °C and 1–40 bar CO_2 pressure for 16 hours using 1 mol% of catalyst **4**. [b] Conversion, % of *trans*-CHC, % of PCHC and % of carbonate linkages determined by ^{1}H NMR spectroscopy of the crude reaction mixture. [c] TON = moles of product/moles of catalyst. [d] TOF = TON/time (h). [e] Determined by GPC relative to polystyrene standards in tetrahydrofuran.

Table 5. Effect of reaction time on the synthesis of poly(cyclohexene carbonate) catalysed by complex **4**[a]

Entry	Time (h)	Conv. (%)[b]	%CHC[b]	%Copolymer (%Carbonate linkage)[b]	TON[c]	TOF[d] (h^{-1})	$M_{n(exp)}$[e](M_w/M_n)[e]
1	2	17	16	84(>99)	14	7.14	2 400 (1.33)
2	5	32	14	86 (>99)	28	5.50	4 500 (1.11)
3	8	49	9	91 (>99)	45	5.57	6 600 (1.14)
4	10	61	12	88 (>99)	54	5.37	7 900 (1.13)
5	15	70	7	93 (>99)	65	4.34	9 400 (1.05)
6	16	72	5	95(>99)	68	4.27	9 500(1.09)

[a] Reactions carried out at 70 ºC and 10 bar CO_2 pressure for 2–16 hours using 1 mol% of catalyst **4**. [b] Conversion, % of trans-CHC, % of PCHC and % of carbonate linkages determined by ^{1}H NMR spectroscopy of the crude reaction mixture. [c] TON = moles of product/moles of catalyst. [d] TOF = TON/time (h). [e] Determined by GPC relative to polystyrene standards in tetrahydrofuran.

3.2.1. Polymer microstructure and end-group analysis of poly(cyclohexene carbonate) produced by complex **4**

The polymer microstructure was analysed by ^{1}H and ^{13}C-NMR spectroscopy (see Figure S7), and MALDI-TOF MS (matrix assisted laser desorption time-of-flight mass spectrometry) to evaluate end-group in the polymers (see Figure 4). Thus, tacticity of the materials was examined by ^{13}C NMR spectroscopy through the analysis of carbonyl region, which resulted atactic polymers since isotactic (153.7 ppm) and syndiotactic (153.7–153.0 ppm) diads were identified (see Figure S7b).

In addition, MALDI-TOF MS spectrum were acquired employing dithranol as matrix and NaOAc as cationization agent. A PCHC distribution including three end-group series of peaks separated by a molecular mass of 142 Da was identified in the spectrum, indicating different initiation possibilities by complex **4**, with the loss of a cyclohexene carbonate unit ($C_7H_{10}O_3$) in all polymer chains (see Figure 4). Particularly, it was established a major series possessing two hydroxyl end groups in the polycarbonate (♦), another series bearing one thioaryloxide group and one hydroxyl end-group (●) and a third series containing one cyclohexenyl group and one hydroxyl end-group (♦), which suggest that chain transfer reactions take place due to the existence of either adventitious water and/or cyclohexenediol through the polymerization event. This behaviour has also been previously observed [51,66,67].

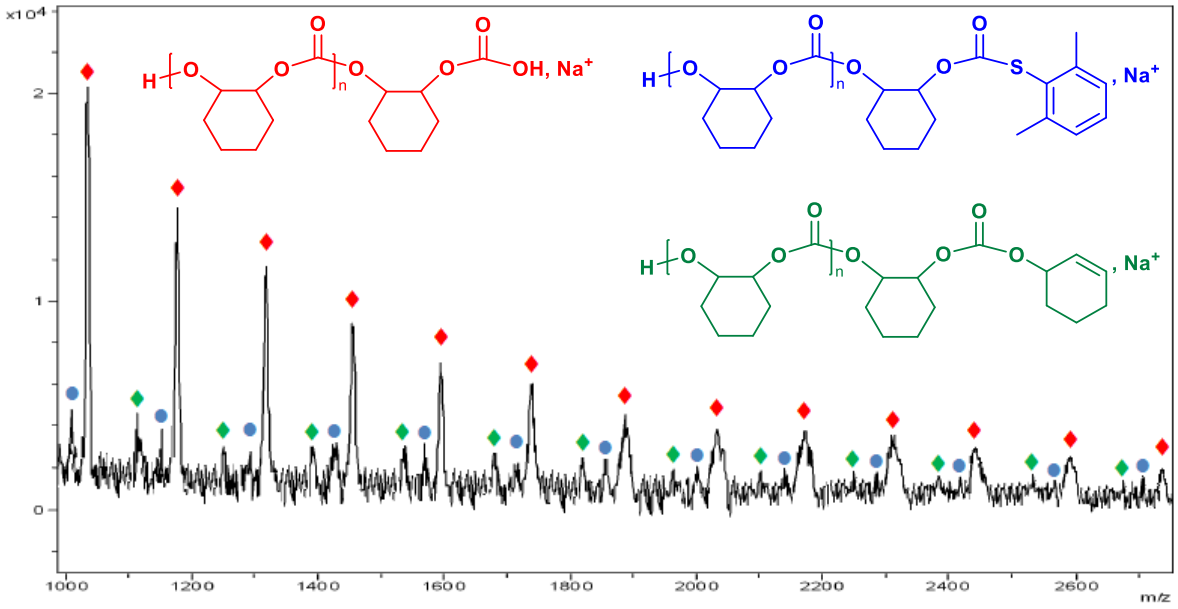

Figure 4. MALDI-ToF mass spectrum of poly(cyclohexene carbonate) sample from Table 4 (entry 2) using zinc complex **4** as catalyst at 70 °C and 10 bar CO_2. Series ♦ has a repeat unit m/z = 1+ (142.07 × DP_{n+1}) + 17 + 22.98, where n = 6-18. Series ● has a repeat unit m/z = 1+ (142.07 × DP_{n+1}) + 137.14 + 22.98, where n = 5-17. Series ♦ has a repeat unit m/z = 1+ (142.07 × DP_{n+1}) + 97.05 + 22.98, where n = 6-17.

4. Conclusions

In summary, we have prepared a series of mono- and dinuclear chiral alkoxide/thioalkoxide scorpionate complexes based on an inexpensive and non-toxic metal. These families of complexes present an interesting variety of structural arrangements, with the scorpionate ligands in different types of coordination modes, which have been unambiguously elucidated by X-ray diffraction studies.

These complexes can act as efficient catalysts for the synthesis of poly(cyclohexene carbonate) via ring-opening copolymerization of cyclohexene oxide and carbon dioxide in the absence of a co-

catalyst. More interestingly, catalytic efficiency is highly dependent on catalyst nuclearity and substituents. Thus, this new approach has led to develop an interesting dinuclear thioalkoxide zinc scorpionate [Zn(bpzaepe)$_2${Zn(SAr)$_2$}] (**4**) that behaves as an effective and selective initiator for poly(cyclohexene carbonate) production under milder conditions. Thus, catalyst **4** shows high catalytic activity (72% conversion and TOF up to 4.3 h^{-1}), carbonate linkage (>99%) and polycarbonate selectivity (95%), at 70 °C, 10 bar of CO_2 pressure after 16 h, under solvent-free conditions, which constitutes a further step forward in the development of inexpensive, more efficient and non-toxic metal-based catalysts for the CO_2 fixation into the selective production of poly(cyclohexene carbonate) with narrow dispersities [17-25,51].

Supplementary Materials: The following are available online at www.mdpi.com/xxx/s1, Figures S1–S3: ^{1}H and ^{13}C-^{1}H NMR spectra of complexes **2**, **4** and **6**, Figure S4: ORTEP view of the complex [Zn(2,6-$Me_2C_6H_3S)_2$(bpzaepeH)] **6**, Table S1: Crystal data and structure refinement for **4**, **5** and **6**, Table S2: Effect of catalyst loading on the synthesis of poly(cyclohexene carbonate) catalysed by complex **4**, Figure S5: GPC trace of poly(cyclohexene carbonate) produced by complex **4** at 70 °C and 10 bar CO_2, Figure S6: Kinetic plot for ring-opening copolymerisation of cyclohexene oxide and carbon dioxide catalysed by complex **4** at 70 °C and 10 bar CO_2, Figure S7: ^{1}H NMR and ^{13}C-{^{1}H} NMR spectra of poly(cyclohexene carbonate) sample prepared using complex **4** at 70 °C and 10 bar CO_2.

Author Contributions: Conceptualization, J.F-B. and L.F.S-B.; Data curation, S.S., M.N. and A.M.R.F.; Formal analysis, A.L-S., A.G. and J.A.C-O.; Investigation, S.S. and M.N.; Resources, J.F-B., L.F.S-B., A.L-S., A.G. and J.A.C-O.; Supervision, J.F-B and L.F.S-B.; Writing—original draft, J.F-B. and L.F.S-B.; Writing—review & editing, J.F-B., L.F.S-B, A.L-S., A.G., J.A.C-O and A.M.R.F. All authors have read and agreed to the published version of the manuscript.

Funding: This research was funded by Ministerio de Economía y Competitividad (MINECO), grant number CTQ2017-84131-R. The APC was funded by Ministerio de Economía y Competitividad.

Conflicts of Interest: The authors declare no conflict of interest.

References

1. Grignard, B.; Gennen, S.; Jérôme, C.; Kleij, A.W.; Detrembleur, C. Advances in the use of CO_2 as a renewable feedstock for the synthesis of polymers. *Chem. Soc. Rev.* **2019**, *48*, 16, 4466–4514. https://doi.org/10.1039/C9CS00047J
2. Artz, J.; Müller, T.E.; Thenert, K.; Kleinekorte, J.; Meys, R.; Sternberg, A.; Bardow, A.; Leitner, W. Sustainable conversion of carbon dioxide: an integrated review of catalysis and life cycle assessment. *Chem. Rev.* **2018**, *118*, 434–504. https://doi.org/10.1021/acs.chemrev.7b00435
3. Dabral, S.; Schaub, T. The use of carbon dioxide (CO_2) as a building block in organic synthesis from an industrial perspective. *Adv. Synth. Catal*. 2019, *361*, 223-246. https://doi.org/10.1002/adsc.201801215
4. Poland, S.J.; Darensbourg, D.J. A quest for polycarbonates provided via sustainable epoxide/CO_2 copolymerization processes. *Green Chem.* **2017**, *19*, 4990-5011. https://doi.org/10.1039/C7GC02560B
5. Zhu, Y.; Romain, C.; Williams, C.K. Sustainable polymers from renewable resources. *Nature* **2016**, *540*, 354-362. https://doi.org/10.1038/nature21001
6. Guo, W.; Gómez, J.E.; Cristòfol, À.; Xie, J.; Kleij. A.W. Catalytic transformations of functionalized cyclic organic carbonates. *Angew. Chem., Int. Ed.* 2018, *57*, 13735-13747. https://doi.org/10.1002/anie.201805009
7. Huang, J.; Worch, J.C.; Dove, A.P.; Coulembier, O. Update and challenges in carbon dioxide-based polycarbonate synthesis. *ChemSusChem* **2019**, *13*, 469-487. https://doi.org/10.1002/cssc.201902719
8. Xu, Y.; Lin, L.; Xiao, M.; Wang, S.; Smith, A.T.; Sun, L.; Meng, Y. Synthesis and properties of CO_2-based plastics: Environmentally-friendly, energy-saving and biomedical polymeric materials. *Prog. Polym. Sci*. **2018**, *80*, 163-182. https://doi.org/10.1016/j.progpolymsci.2018.01.006
9. Paul, S.; Romain, C.; Shaw, J.; Williams, C. K. Sequence selective polymerization catalysis: a new route to aba block copoly(ester-b-carbonate-b-ester). *Macromolecules* **2015**, *48*, 6047-6056. https://doi.org/10.1021/acs.macromol.5b01293
10. Chapman, A.M.; Keyworth, C.; Kember, M.R.; Lennox, A.J.J.; Williams, C.K. Adding value to power station captured CO_2: tolerant Zn and Mg homogeneous catalysts for polycarbonate polyol production. *ACS Catal.* **2015**, *5*, 1581-1588. https://doi.org/10.1021/cs501798s
11. Paul, S.; Zhu, Y.; Romain, C.; Brooks, R.; Saini, P.K.; Williams, C.K. Ring-opening copolymerization (ROCOP): synthesis and properties of polyesters and polycarbonates. *Chem. Commun.* **2015**, *51*, 6459-6479. https://doi.org/10.1039/C4CC10113H
12. Sulley, G.S.; Gregory, G.L.; Chen, T.T.D.; Peña-Carrodeguas, L.; Trott, G.; Santmarti, A.; Lee, K.; Terrill, N.J.; Williams, C.K. Switchable catalysis improves the properties of CO_2-derived polymers: Poly(cyclohexene carbonate-b-ε-decalactone-b-cyclohexene carbonate) adhesives, elastomers, and toughened plastics. *J. Am. Chem. Soc.* **2020**, *142*, 4367-4378. https://doi.org/10.1021/jacs.9b13106
13. Song, Q.-W.; Zhou, Z.-H.; He, L.-N. Efficient, selective and sustainable catalysis of carbon dioxide. *Green Chem.* **2017**, *19*, 3707–3728. https://doi.org/10.1039/C7GC00199A
14. Pescarmona, P.P.; Taherimehr, M. Challenges in the catalytic synthesis of cyclic and polymeric carbonates from epoxides and CO_2. *Catal. Sci. Technol.* **2012**, *2*, 2169–2187. https://doi.org/10.1039/C2CY20365K
15. Andrea, K.A.; Kerton, F.M. Triarylborane-catalyzed formation of cyclic organic carbonates and polycarbonates. *ACS Catal.* **2019**, *9*, 1799–1809. https://doi.org/10.1021/acscatal.8b04282
16. Trott, G.; Saini, P.K.; Williams, C.K. Catalysts for CO_2/epoxide ring-opening copolymerization. *Philos. Trans. R. Soc., A Math. Phys Eng. Sci.* **2016**, *374* (2061), 20150085. https://doi.org/10.1098/rsta.2015.0085
17. Pankhurst, J. R.; Paul, S.; Zhu, Y.; Williams, C. K.; Love, J. B. Polynuclear alkoxy–zinc complexes of bowl-shaped macrocycles and their use in the copolymerisation of cyclohexene oxide and CO_2. *Dalton Trans.* **2019**, *48*, 4887–4893. https://doi.org/10.1039/C9DT00595A

18. Reiter, M.; Vagin, S.; Kronast, A.; Jandl, C.; Rieger, B. A Lewis acid β-diiminato-zinc-complex as all-rounder for co- and terpolymerisation of various epoxides with carbon dioxide. *Chem. Sci.* **2017**, *8*, 1876-1882. https://doi.org/10.1039/C6SC04477H
19. Kernbichl, S.; Reiter, M.; Adams, F.; Vagin, S.; Rieger, B. CO_2-Controlled One-Pot Synthesis of AB, ABA Block, and Statistical Terpolymers from β-Butyrolactone, Epoxides, and CO_2. *J. Am. Chem. Soc.* **2017**, *139*, 6787-6790. https://doi.org/10.1021/jacs.7b01295
20. Schütze, M.; Dechert, S.; Meyer, F. Highly Active and Readily Accessible Proline-Based Dizinc Catalyst for CO_2/Epoxide Copolymerization. *Chem. Eur. J.* **2017**, *23*, 16472-16475. https://doi.org/10.1002/chem.201704754
21. Thevenon, A.; Garden, J.A.; White, A.J.P.; Williams, C.K. Dinuclear Zinc Salen Catalysts for the Ring Opening Copolymerization of Epoxides and Carbon Dioxide or Anhydrides. *Inorg. Chem.* **2015**, *54*, 11906–11915. https://doi.org/10.1021/acs.inorgchem.5b02233
22. Kissling, S.; Lehenmeier, M.W.; Altenbuchner, P.T.; Kronast, A.; Reiter, M.; Deglmann, P.; Seemann, U.B.; Rieger, B. Dinuclear zinc catalysts with unprecedented activities for the copolymerization of cyclohexene oxide and CO_2. *Chem. Commun*. **2015**, *51*, 4579–4582. https://doi.org/10.1039/C5CC00784D
23. Kissling, S.; Altenbuchner, P.T.; Lehenmeier, M.W.; Herdtweck, E.; Deglmann, P.; Seemann, U.B.; Rieger, B. Mechanistic aspects of a highly active dinuclear zinc catalyst for the co-polymerization of epoxides and CO_2. *Chem. Eur. J.* **2015**, *21*, 8148–8157. https://doi.org/10.1002/chem.201406055
24. Kember, M.R.; Knight, P.D.; Reung, P.T.R.; Williams, C.K. Highly active dizinc catalyst for the copolymerization of carbon dioxide and cyclohexene oxide at one atmosphere pressure. *Angew. Chem. Int. Ed*. **2009**, *48*, 931–933. https://doi.org/10.1002/anie.200803896
25. Moore, D.R.; Cheng, M.; Lobkovsky, E.B.; Coates, G.W. Electronic and steric effects on catalysts for CO_2/epoxide polymerization: subtle modifications resulting in superior activities. *Angew. Chem. Int. Ed.* **2002**, *41*, 2599–2602. https://doi.org/10.1002/1521-3773(20020715)41:14<2599::AID-ANIE2599>3.0.CO;2-N
26. Ni, K.; Kozak, C.M. Kinetic studies of copolymerization of cyclohexene oxide with CO_2 by a diamino-bis(phenolate) chromium(iii) complex. *Inorg. Chem.* **2018**, *57*, 3097-3106. https://doi.org/10.1021/acs.inorgchem.7b02952
27. Castro-Osma, J.A.; Lamb; K.J. North, M. Cr(salophen) complex catalyzed cyclic carbonate synthesis at ambient temperature and pressure. *ACS Catal.* **2016**, *6*, 5012-5025. https://doi.org/10.1021/acscatal.6b01386
28. Viciano, M.; Munoz, B.K.; Godard, C.; Castillon, S.; Reyes, M.L.; Garcia-Ruiz, M.; Claver, C. Salcy-naphthalene cobalt complexes as catalysts for the synthesis of high molecular weight polycarbonates. *ChemCatChem* **2017**, *9*, 3974-3981. https://doi.org/10.1002/cctc.201701250
29. Hatazawa, M.; Nakabayashi, K.; Ohkoshi, S.; Nozaki, K. In situ generation of Co^{III}–Salen complexes for copolymerization of propylene oxide and CO_2. *Chem. Eur. J.* **2016**, *22*, 13677-13681. https://doi.org/10.1002/chem.201602546
30. Andrea, K.A.; Butler, E.D.; Brown, T.R.; Anderson, T.S.; Jagota, D.; Rose, C.; Lee, E.M.; Goulding, S.D.; Murphy, J.N.; Kerton, F.M.; Kozak, C.M. Iron complexes for cyclic carbonate and polycarbonate formation: selectivity control from ligand design and metal-center geometry. *Inorg. Chem.* **2019**, *58*, 11231−11240. https://doi.org/10.1021/acs.inorgchem.9b01909
31. Gu, G.-G.; Yue, T.-J.; Wan, Z.-Q.; Zhang, R.; Lu, X.-B.; Ren, W.-M. A Single-site iron(III)-salan catalyst for converting COS to sulfur-containing polymers. *Polymers* **2017**, *9*, 515. https://doi.org/10.3390/polym9100515
32. Hua, L.; Li, B.; Han, C.; Gao, P.; Wang, Y.; Yuan, D.; Yao, Y. Synthesis of homo- and heteronuclear rare-earth metal complexes stabilized by ethanolamine-bridged bis(phenolato) ligands and their application in

catalyzing reactions of CO_2 and epoxides. *Inorg. Chem.* **2019**, *58*, 8775–8786. https://doi.org/10.1021/acs.inorgchem.9b01169

33. Wang, L.; Xu, C.; Han, Q.; Tang, X.; Zhou, P.; Zhang, R.; Gao, G.; Xu, B.; Qin, W.; Liu, W. Ambient chemical fixation of CO_2 using a highly efficient heterometallic helicate catalyst system. *Chem. Commun.* **2018**, *54*, 2212-2215. https://doi.org/10.1039/C7CC09092G
34. Wang, Y.; Zhao, Y.J.; Ye, Y.S.; Peng, H.Y.; Zhou, X.P.; Xie, X.L.; Wang, X.H.; Wang, F.S. A one-step route to CO_2-based block copolymers by simultaneous ROCOP of CO_2/epoxides and RAFT polymerization of vinyl monomers. *Angew. Chem., Int. Ed.* **2018**, *57*, 3593-3597. https://doi.org/10.1002/anie.201710734
35. Kindermann, N.; Cristofol, A.; Kleij, A.W. Access to biorenewable polycarbonates with unusual glass-transition temperature (T_g) modulation. *ACS Catal.* **2017**, *7*, 3860-3863. https://doi.org/10.1021/acscatal.7b00770
36. Shaikh, R.R.; Pornpraprom, S.; D'Elia, V. Catalytic strategies for the cycloaddition of pure, diluted, and waste CO_2 to epoxides under ambient conditions. *ACS Catal.*, **2018**, *8*, 419–450. https://doi.org/10.1021/acscatal.7b03580
37. Deacy, A.C.; Kilpatrick, A.F.R.; Regoutz, A.; Williams, C.K. Understanding metal synergy in heterodinuclear catalysts for the copolymerization of CO_2 and epoxides. *Nat. Chem.* **2020**, *12*, 372–380.
38. Trott, G.; Garden, J.A.; Williams, C.K. Heterodinuclear zinc and magnesium catalysts for epoxide/CO_2 ring opening copolymerizations. *Chem. Sci.* **2019**, *10*, 4618-4627. https://doi.org/10.1039/C9SC00385A
39. July: Carbon Dioxide, http://www.novomer.com/? action=CO2 (accessed July 2020).
40. Empower Materials http://www.empowermaterials.com (accessed July 2020).
41. Ok, M.-A.; Jeon, M. Properties of poly(propylene carbonate) produced via SK Energy's Greenpol™ Technology, ANTEC **2011**, Society of Plastics Engineers, Econic Technologies, http://www.econic-technologies.com/ (accessed July 2020).
42. Suter, P.M.; Wood, R.J.; Russell, R.M. Mineral requirements of elderly people. *Am. J. Clin. Nutr.* **1995**, *62*, 493–505. https://doi.org/10.1093/ajcn/62.3.493
43. Turnlund, J.R.; Betschart, A.A.; Liebman, M.; Kretsch, M.J.; Sauberlich, H.E. Vitamin B–6 depletion followed by repletion with animal- or plant-source diets and calcium and magnesium metabolism in young women. *Am. J. Clin. Nutr.* **1992**, *56*, 905–910. https://doi.org/10.1093/ajcn/56.5.905
44. Nakanishi, T. Potential toxicity of organotin compounds *via* nuclear receptor signaling in mammals. *J. Health Sci.* **2007**, *53*, 1–9. https://doi.org/10.1248/jhs.53.1
45. Appel, K.E. Organotin Compounds: toxicokinetic Aspects. *Drug Metab. Rev.* **2004**, *36*, 763–786. https://doi.org/10.1081/DMR-200033490
46. Otero, A.; Fernández-Baeza, J.; Lara-Sánchez, A.; Sánchez-Barba, L.F. Metal complexes with heteroscorpionate ligands based on the bis(pyrazol-1-yl)methane moiety: Catalytic chemistry. *Coord. Chem. Rev.* **2013**, *257*, 1806–1868. https://doi.org/10.1016/j.ccr.2013.01.027
47. Honrado, M.; Otero, A.; Fernández-Baeza, J.; Sánchez-Barba, L.F.; Garcés, A.; Lara-Sánchez, A.; Rodríguez, A. M. Copolymerization of cyclic esters controlled by chiral NNO-scorpionate zinc initiators. *Organometallics* **2016**, *35*, 189–197. https://doi.org/10.1021/acs.organomet.5b00919
48. Honrado, M.; Otero, A.; Fernández-Baeza, J.; Sánchez-Barba, L.F.; Garcés, A.; Lara-Sánchez, A.; Rodríguez, A.M. Synthesis and dynamic behavior of chiral NNO-scorpionate zinc initiators for the ring-opening polymerization of cyclic esters. *Eur. J. Inorg. Chem.* **2016**, 2562–2572. https://doi.org/10.1002/ejic.201501347
49. Honrado, M.; Otero, A.; Fernández-Baeza, J.; Sánchez-Barba, L.F.; Garcés, A.; Lara-Sánchez, A.; Martínez-Ferrer, J.; Sobrino S.; Rodríguez A.M. New racemic and single enantiopure hybrid

583 scorpionate/cyclopentadienyl magnesium and zinc initiators for the stereoselective ROP of lactides.
584 *Organometallics* **2015**, *34*, 3196-3208. https://doi.org/10.1021/acs.organomet.5b00248
585 50. Honrado, M.; Otero, A.; Fernandez-Baeza, J.; Sanchez-Barba, L.F.; Garcés, A.; Lara-Sanchez, A.; Rodriguez,
586 A.M. Enantiopure N,N,O-scorpionate zinc amide and chloride complexes as efficient initiators for the
587 heteroselective ROP of cyclic esters. *Dalton Trans.* **2014**, *43*, 17090–17100.
588 https://doi.org/10.1039/C4DT02178A
589 51. Martínez, J.; Castro-Osma, J.A.; Lara-Sánchez, A.; Otero, A.; Fernández-Baeza, J.; Tejeda, J.; Sánchez-Barba,
590 L.F.; Rodríguez-Diéguez, A. Ring-opening copolymerisation of cyclohexene oxide and carbon dioxide
591 catalysed by scorpionate zinc complexes. *Polym. Chem.* **2016**, *7*, 6475–6484.
592 https://doi.org/10.1039/C6PY01559J
593 52. Sobrino, S.; Navarro, M.; Fernández-Baeza, J.; Sánchez-Barba, L.F.; Garcés, A.; Lara-Sánchez, A.; Castro-
594 Osma, J.A. Efficient CO_2 fixation into cyclic carbonates catalyzed by NNO-scorpionate zinc complexes.
595 *Dalton Trans.* **2019**, *48*, 10733-10742. https://doi.org/10.1039/C9DT01844A
596 53. Otero, A.; Fernández-Baeza, J.; Sánchez-Barba, L.F.; Sobrino, S.; Garcés, A.; Lara-Sánchez, A.; Rodríguez,
597 A.M. Mono- and binuclear chiral N,N,O-scorpionate zinc alkyls as efficient initiators for the ROP of rac-
598 lactide. *Dalton Trans.* **2017**, *46*, 15107-15117. https://doi.org/10.1039/C7DT03045B
599 54. SAINT v8.37, Bruker-AXS, APEX3 v2016.1.0. Madison, Wisconsin, USA. 2016.
600 55. SADABS, Krause, L., Herbst-Irmer, R., Sheldrick, G.M. & Stalke, D. Comparison of silver and molybdenum
601 microfocus X-ray sources for single-crystal structure determination. *J. Appl. Crystallogr.* **2015**, *48*, 3-10.
602 https://doi.org/10.1107/S1600576714022985
603 56. Farrugia, L.J. WinGX and ORTEP for Windows: an update. *J. Appl. Cryst.* **2012**, *45*, 849-854.
604 https://doi.org/10.1107/S0021889812029111
605 57. Sheldrick, G. M. SHELX-2014, Program for Crystal Structure Refinement, University of Göttingen,
606 Göttingen, Germany, 2014.
607 58. Sluis, P.V.D.; Spek, A. L. BYPASS: an effective method for the refinement of crystal structures containing
608 disordered solvent regions. *Acta Crystallogr., Sect. A: Found. Crystallogr.*, **1990**, *46*, 194-201.
609 https://doi.org/10.1107/S0108767389011189
610 59. Timothy, J.B.; Pratt III, H.D.; Alam, T.M.; Headley, T.; Rodriguez, M.A. Synthesis and characterization of
611 thiolate-oxo ligated zinc alkyl derivatives for production of Zn-based nanoparticles. *Eur. J. Inorg. Chem.*
612 **2009**, 855–865. https://doi.org/10.1002/ejic.200800886
613 60. Grunova, E.; Roisnel, T.; Carpentier, J.-F. Zinc complexes of fluorous alkoxide-iminoligands: Synthesis,
614 structure, and use in ring-opening polymerization of lactide and β-butyrolactone. *Dalton Trans*. **2009**, 9010–
615 9019. https://doi.org/10.1039/B902087J
616 61. Poirier, V.; Roisnel, T.; Carpentier, J.-F.; Sarazin, Y. Versatile catalytic systems based on complexes of zinc,
617 magnesium and calcium supported by a bulky bis(morpholinomethyl)phenoxy ligand for the large-scale
618 immortal ring-opening polymerisation of cyclic esters. *Dalton Trans*. **2009**, 9820–9027.
619 https://doi.org/10.1039/B917799J
620 62. Johnson, A.L.; Hollingsworth, N.; Kociok-Köhn, G.; Molloy, K.C. Organozinc aminoalcoholates: synthesis,
621 structure, and materials chemistry. *Inorg. Chem.* **2008**, *47*, 12040–12048. https://doi.org/10.1021/ic801591d
622 63. Otero, A.; Fernández-Baeza, J.; Sánchez-Barba, L.F.; Tejeda, J.; Honrado, M.; Garcés, A.; Lara-Sánchez, A.;
623 Rodríguez, A.M. Chiral N,N,O-scorpionate zinc alkyls as effective and stereoselective initiators for the
624 living ROP of lactides. *Organometallics,* **2012**, *31*, 4191–4202. https://doi.org/10.1021/om300146n

625 64. Alonso-Moreno, C.; Garcés, A.; Sánchez-Barba, L.F.; Fajardo, M.; Fernández-Baeza, J.; Otero, A.; Antiñolo,
626 A.; Lara-Sánchez, A.; Broomfield, L.; López-Solera, I.; Rodríguez, A.M. Discrete heteroscorpionate lithium
627 and zinc alkyl complexes. synthesis, structural studies, and ROP of cyclic esters. *Organometallics* **2008**, *27*,
628 1310–1321. https://doi.org/10.1021/om701187s
629 65. Paradiso, V.; Capaccio, V.; Lamparelli, D.H.; Capacchione, C. Metal complexes bearing sulfur-containing
630 ligands as catalysts in the reaction of CO_2 with epoxides. *Catalysts*, **2020**, *10*, 825.
631 https://doi.org/10.3390/catal10080825
632 66. Kember, M.R.; Williams, C.K. Efficient magnesium catalysts for the copolymerization of epoxides and CO_2;
633 using water to synthesize polycarbonate polyols. *J. Am. Chem. Soc.*, **2012**, *134*, 15676–15679.
634 https://doi.org/10.1021/ja307096m
635 67. Xiao, Y.; Wang, Z.; Ding, K. Intramolecularly dinuclear magnesium complex catalyzed copolymerization
636 of cyclohexene oxide with CO_2 under ambient CO_2 Pressure: kinetics and mechanism. *Macromolecules* **2006**,
637 *39*, 128–137. https://doi.org/10.1021/ma051859+

638